Journal of Engineering for Industry, ASME, New York, NY, Vol. 118, No. 1, 1996, pp. 37-44.

SPREAD SHEET MODEL OF CONTINUOUS CASTING

Brian G. Thomas and Bryant Ho

University of Illinois at Urbana-Champaign
Department of Mechanical and Industrial Engineering
1206 W. Green Street,
Urbana, IL 61801

Abstract

Spreadsheet programs, such as Microsoft Excel, Informix WINGZ, and Lotus 123 provide a framework for very fast and easy development of simple engineering models. The present paper describes a model of the continuous casting process that has been developed using a spreadsheet program, Microsoft Excel, running on a Macintosh II personal computer. The model consists of two-dimensional (2-D) steady-state finite-difference heat conduction calculations within a continuous casting mold coupled to a one-dimensional (1-D) transient solidification heat transfer model of the solidifying shell. The model structure and equations are described and the model predictions are compared with previous solutions. Practical examples using the model are discussed and sample results are provided. Spreadsheet programs running on fast personal computers are capable of relatively complex calculations that would require extensive effort using conventional programming languages.

Introduction

Mathematical models can be used to gain valuable insight into complex process phenomena. For example, in the continuous casting process, the temperature history of the solidifying steel shell is very important to the ultimate quality of the product (Mahapatra et al., 1991). Heat transfer across the interface between the solidifying steel shell and the copper mold controls this temperature distribution (Jenkins et al., 1994). Defects have been linked to mold temperature variations (Jenkins et al., 1994) and the position of defects beneath the shell surface corresponds to the temperature when they were created (Szekely et al, 1988). A mathematical model of heat conduction across the shell, interface, and mold, based on finite difference or finite element methods, is a useful tool to understand and solve these problems (Mahapatra et. Al. 1991; Szekely et al., 1988).

To develop models such as this, sophisticated computer programs are usually written in a compiled language such as FORTRAN. These programs require significant effort to create, modify, and maintain. Partly because of this complexity, most previous heat flow models of continuous casting uncouple the calculation of temperature in the mold and shell using separate programs. Heat transfer across the mold / shell interface is calibrated with experimental measurements and transferred between programs by hand (Mahapatra et al, 1991; Szekely et al., 1988).

A comprehensive system of finite element models of fluid flow, heat transfer, and stress are being developed to understand and investigate the formation of defects in the mold region of continuous steel slab casters (Thomas, 1989). These models include the effects of mold distortion, the influence of fluid flow in the liquid pool on solidification of the shell, and coupling between shrinkage of the shell and the reduction of heat transfer across the interface due to air gap formation. Calibrating these models requires program modifications and numerical experiments that are expensive, time consuming and tedious. To speed up this testing, simplified models were sought, that would be easy to create and modify. These simple models would serve many other purposes also.

The present work was undertaken to develop a fast, simple, and flexible model of two-dimensional (2-D) steady-state heat conduction within the mold, coupled with a one-dimensional (1-D) transient heat flow model of solidification of the steel shell, as it moves down through the mold. This paper describes the formulation of this model, which has been implemented using commercial spreadsheet programs (Microsoft EXCEL and Informix WINGZ) on a MacIntosh II personal computer.

Model Formulation

Figure 1 shows a schematic of the continuous casting process. Metal flows via gravity from a holding tundish down through a submerged entry nozzle into a mold cavity. The liquid steel solidifies against the four walls of the water-cooled copper mold, and forms a steel shell that acts as a container for the liquid as it is withdrawn continuously from the mold bottom. Mold powder is added to the free surface of the liquid steel, and melts into a flux which flows between the solid steel shell and the mold wall, where it acts as a lubricant. This flux controls heat flow across the interface according to its thickness and thermal properties. Calculating this heat flow, and the resulting temperature distribution in the mold and steel shell, is the objective of the present model.

Construction of a usable spread sheet model begins with a top section, which contains the values of input variables and constants, with appropriate labels (including units) in the adjoining cells. The lower portion of the spread sheet contains columns of cell equations, which are oriented in a logical manner with an appropriate title above each column. Cell equations are constructed using the input variable cells in the top section. This format is important to allow for easy parametric investigation. Simply changing a single number in the top section enables complete recalculation of the spread sheet model under the new condition.

Figure 2 presents the structure of the spreadsheet model and its typical contents. Figure 2 a) schematically illustrates the sections that make up the spreadsheet and indicates the letters of the figures that detail typical contents of the cells in each section. Figure 2 shows that the spreadsheet looks similar to the continuous casting process being simulated. The calculated temperatures in the mold and steel are displayed in rectangular sections where they would be expected. As detailed in Figure 2 c), they are separated by a column of cells representing the interface between the mold and shell. A column of cells containing the mold cooling water temperatures is found on the left side of the mold. This natural format, which is possible for any model with 2-D results, greatly facilitates creation of the spreadsheet and examination of the results.

Copper Mold Model

Two dimensional, steady state temperatures within a rectangular section through the mold were calculated by solving:

$$k\left(\frac{\partial^2 T}{\partial x^2} + \frac{\partial^2 T}{\partial y^2}\right) = 0 \qquad (1)$$

Each cell in the mold region of the spreadsheet is treated as a node in a finite difference discretization of this equation. This produces classic equations for the temperature within each interior cell as a function of the temperatures of the adjacent cells (Minkowycz et. al. 1988) :

$$T_{cell} = \frac{T_W\,\Delta y^2 + T_E\,\Delta y^2 + T_S\,\Delta x^2 + T_N\,\Delta x^2}{2(\Delta y^2 + \Delta x^2)} \qquad (2)$$

The standard notation used for the subscripts that describe the relative position of the adjacent cells is given in Figure 3.

Equations for the cells comprising the mold boundaries are given in Appendix I. It is easy to modify and copy these cell equations around in the spreadsheet in order to make changes to the boundary conditions, lengthen the mold, or change the mesh size as desired. Results are equally easy to visualize, understand, and modify because each cell contains both the nodal equation and its calculated temperature. Figure 2 c) shows typical results of mold cell temperatures.

Input variables and constants that are used throughout the spreadsheet, are stored once in the top region of the spreadsheet, shown in Figure 2 b). This data includes the casting conditions, thermal properties of the mold and steel materials, and mesh and time step parameters.

Solution Methodology:

The only solution method provided by most spreadsheet programs is successive substitution, where calculation sweeps through the spreadsheet cells from left to right and top row to bottom row, using the most current values for the calculations at all times. Solving for the mold temperatures therefore requires several complete sweeps or iterations, since the cell temperatures depend implicitly upon each other. Fortunately, this simple point by point solution method is powerful enough to solve many problems, including the present system of finite difference equations.

While entering cell equations into the spreadsheet, automatic calculation (updating of the cells) is turned off. After creating the interior cell equation and copying it to fill the mold region, the temperatures of all boundary cells are fixed to constant values. An "initial guess" solution is performed by selecting "calculate now" from the menu. The calculation automatically "sweeps" through the spreadsheet for the requested number of iterations or until a convergence criterion is satisfied. Once reasonable temperatures are achieved, the more sophisticated boundary conditions provided in Appendix I are implemented by changing the boundary cell equations. The spreadsheet thus evolves, as the model "programming" and "execution" stages proceed together.

Instability of the spreadsheet calculation is easily spotted by watching the cells update. Cells with unreasonable or unstable equations exhibit drastic temperature oscillations, which propagate to the surrounding neighbors. When this happens, calculations are immediately stopped and the "bad" cells are overwritten with temperatures from other "good" cells in the spreadsheet. After the bug is found and corrected, calculation is restarted.

The calculations tend to become less stable as the boundary conditions are changed from fixed temperature to convection coefficient to specified heat flux. The coupling between the cells in the vertical direction also makes convergence more difficult. Thus, a 1-D heat flow relationship was used for cells below the upper “meniscus region” of the mold, where axial conduction is not very important. These optional cell equations are given in Appendix I. Eqs. 2, 4, and 6.

Convergence is usually steady but can be slow, so iterations were continued until a strict criterion was met: the maximum temperature change in any cell must be less than 0.02 ˚C between successive iterations. The mold model requires the most execution time, typically needing 50 iterations or 600 CPU s for 816 cells (6 x 136 grid) using Microsoft Excel 3.0 on a MacIntosh II. Execution time increases roughly linearly with the number of cells.

Steel Shell Solidification Model

To model solidification and temperature of the steel shell as it moves down through the mold, an enthalpy formulation of the transient 1-D heat conduction equation is solved:

$$\rho \frac{\partial H}{\partial t} = k \frac{\partial^2 T}{\partial x^2} \tag{3}$$

Using a simple explicit time stepping algorithm and a 1-D finite difference discretization, the enthalpy of a typical interior node is described in terms of its enthalpy at the previous time step (found in the cell above) as :

$$H_{cell} = H_N + \frac{k\Delta t}{\rho \Delta x^2}\left(T_{NE} - 2\,T_N + T_{NW}\right) \tag{4}$$

This equation requires the previously calculated temperatures of this node and its neighbors at the previous time step. A simple relationship, shown in Figure 4, was used to relate temperature and enthalpy, assuming a unique freezing temperature and constant Cp. Using this relationship, a cell temperature can be calculated from its enthalpy in a single unified expression:

$$T_{cell} = \min\left[\frac{H_{cell}}{C_p}, \max\left\{\frac{H_{cell} - L_f}{C_p}, T_{sol}\right\}\right] \tag{5}$$

This temperature can only be calculated after the enthalpy is known. Thus, it is easier, and computationally more efficient, to construct the spreadsheet if the enthalpy of each node is calculated and stored completely within its own single cell. This can be accomplished by substituting Eq. 5 three times into Eq. 4, to produce the long, but straight forward equation given in Appendix I Eq. 12. The advantage is a unified "enthalpy section" of the spreadsheet where the calculations for each node depend only upon cell values found in the row above, so are stable.

To present the results, the temperature of each enthalpy cell is recalculated in a single corresponding temperature cell using Eq. 5 (or Equation 14 in Appendix I). For legibility, this equation (and its result) is stored in a separate temperature section of the spreadsheet, created adjacent to the mold section, as shown in Figure 2 c). The enthalpy section is stored further away and typical results are shown in Figure 2 h).

For initial conditions, the top row of cells are simply set to the pour temperature defined in the input part of the spreadsheet. The cell equations for both enthalpy and temperature for all types of nodes required for the continuous casting simulation are given in Appendix I.

Since this model is explicit, no iteration is required. Thus, the spreadsheet is converged after the first iteration, if the shell is uncoupled from the mold. For the same number of cells, (ie. mesh size) the solidification model converges faster than the mold model. There is, however, a well-known theoretical restriction on the time step and mesh size combinations possible to achieve stable convergence for linear problems (Minkowycz et al. 1988):

$$\frac{k}{\rho C_p}\frac{\Delta t}{\Delta x^2} < 0.5 \tag{6}$$

The time step size was restricted even more for the nonlinear solidification problem at hand. The mesh employed for the solidification model depends upon the purpose of the model. When the mold region is of interest, a fine (2 mm) spacing is used between nodes, requiring a small time step. However, there is no need to create cells for the entire slab section, which is mainly liquid. When the later stages of solidification below the mold, or the final point of solidification is important, all of the liquid must be modeled, but a courser node spacing and larger time step can be used.

Coupling

The mold and shell models are useful tools when run separately, but are even more powerful when coupled together. Coupling between the models is achieved by letting the mesh size of the mold in the casting direction, Δy, depend on the time step size used in the steel, Δt, and the casting speed, v:

$$\Delta y = v\,\Delta t \tag{7}$$

Distance below the meniscus, y, is accumulated in the same way as many other variables in the spreadsheet:

$$y_{cell} = y_N + \Delta y \tag{8}$$

In addition, heat transfer between the mold and steel is defined by:

$$q'' = h_{gap}\,(T_{shell\ surface} - T_{mold\ hot\ face}) \tag{9}$$

Various functions for h_{gap} are being explored. When simulating a slice through the wide face, liquid pressure ensures good contact between the shell and mold and prevents any air gaps due to shrinkage. Heat transfer is governed by conduction and radiation across the transparent powder layers. Figure 2 g) shows the results obtained with the following equation, which was used to produce the typical results given in the rest of Figure 2:

$$h_{gap} = 1/\left(\frac{1}{h_{mold/flux\ contact}} + \frac{\Delta x_{air}}{k_{air}} + \frac{\Delta x_{flux}}{k_{flux}} + \frac{1}{h_{flux/shell\ contact}}\right) + \sigma\,\varepsilon\,(T^2_{shell\ surface} + T^2_{mold\ hot\ face})\,(T_{shell\ surface} + T_{mold\ hot\ face}) \tag{10}$$

The solution algorithm was found to produce stable results for this coupled simulation, but depends upon starting from a reasonable guess. This is best achieved by modifying a previously converged spreadsheet.

Model Verification

The models were verified independently by uncoupling them from each other by simply changing the equations in the boundary cells representing the mold and shell surfaces. Model predictions were compared successfully with analytical solutions from Carslaw and Jaeger (1959) employing fixed temperature boundary conditions, to verify their internal consistency.

The solidification model was then further verified by using it to reproduce predictions of temperature and shell thickness from two previously-published 1-D transient models of continuous casting. This required fixing the heat flux leaving the steel surface cells to prescribed values. This was accomplished using a heat flux versus time "look-up table", shown in Figure 2f), to define q" in Eq. 11 in Appendix I. Heat flux values for the cells in the spreadsheet column representing the interface were then based on piece-wise linear interpolation between pairs of points (y, q") in the look-up table:

$$q''_{cell} = q''_1 + \frac{y - y_1}{y_2 - y_1} * (q''_2 - q''_1) \qquad (11)$$

The appropriate y_1 and y_2 values were found automatically for the current distance, y, using the INDEX function and the corresponding q''_1 and q''_2 values were found by the VLOOKUP function in Excel 3.0. This look-up table procedure provides a convenient, flexible method to input a variety of data into the model.

The previous models used in the comparison employed an integral profile method (Hills, 1969) and an explicit finite difference method implemented into a FORTRAN program (Lait et al. 1974). Table I shows the steel property data and casting conditions used in the previous work and their approximation for the spreadsheet model. Note that both the liquidus and pour temperatures were decreased by 61 °C in the present work in order to simultaneously satisfy the requirement of a unique solidification temperature and maintain a constant superheat of 20 °C.

Shell thickness was inferred by assuming the solid front was positioned at the boundary between adjacent cells at the time each cell just cooled below the solidification temperature. Figure 5 compares the shell thickness profile predicted with the spreadsheet model with two results from previous published models of continuous casting. The spreadsheet results are seen to fall between the previously published curves. This agreement suggests that the modeling assumptions and procedure are reasonable. In particular, a unique solidification temperature, which is attractive for low alloy steels with a narrow solidification range, can even approximate the solidification of a stainless steel.

Model Applications

The verified model can be used for many purposes. For example, the variation in mold copper thickness between the inside and outside radius resulting from mold curvature affects the mold temperatures. The magnitude of this effect was investigated by varying the mold thickness with distance down the mold, using the machine radius. This was easy to incorporate into the model by inserting two new columns into the spreadsheet to calculate and store the local mold thickness and corresponding Δx for each row of cells. (See Figure 2 d).

Boiling in the water channels is a serious potential quality problem. The model was modified to check if boiling is likely under particular mold and casting conditions of interest. This required

enhancing the model to improve calculation of the mold water heat transfer coefficient. Relationships from Burmeister (1983) were incorporated in a separate section of the spreadsheet to calculate h_{water} as a function of mold cooling water velocity and temperature, as shown in Figure 2 e). Knowing the mass flow rate through each cooling water channel, M_{water}, and the distance between channels, W_{water}, from the input data section, the increase in water temperature as it flows up the mold was calculated:

$$T_{water\ cell} = T_S + \frac{q''_{mold\ cold\ face} * W_{water} * \Delta y}{M_{water} * C_{pwater}} \qquad (12)$$

This equation is also useful for calculating the overall increase in water temperature, for comparison with measurements on operating casters.

Spray heat transfer was introduced below the mold by copying more cells to extend the steel shell downward and changing the cells containing the q" boundary condition to simulate spray water heat flux. This enables the model to simulate phenomena such as reheating of the shell surface below the mold, which is important for designing spray water cooling systems to avoid surface crack formation.

Another use of the model is to approximate the ideal taper of the narrow-face mold walls needed to match the shrinkage of the shell. This is readily calculated in a single cell based on the predicted shell surface temperature at mold exit:

$$\text{Ideal \% taper / m} = \frac{\alpha\ (T_{sol} - T_{surface\ node\ at\ mold\ exit})}{L} \qquad (13)$$

where α is the thermal expansion coefficient of the steel and L is the effective mold length. This ideal taper varies as a function of casting conditions, such as casting speed, grade, and interface heat transfer parameters. Despite the tremendous simplification inherent in this equation, the predictions match casting operation experience quite reasonably.

Finally, the model has been used to develop a better understanding of the interaction between the mold and the shell, (Ho, 1992). For example, if the mold "flux", which fills most of the gap, is allowed to cool completely below its solidification temperature, then it becomes viscous and is less able to lubricate the strand. This increases mold friction and makes problems such as surface cracks more likely. Once calibrated, this phenomenon can be predicted using the model.

The many input parameters to the model must be calibrated using data from casting operations, such as mold thermocouple measurements, mold water temperature rise, shell thicknesses from breakout shells, and mold powder thicknesses. This requires significant trial and error, including different functions for heat flow across the interface, Eq. (10). In future work, these calibrated parameters and functions can be used in the more sophisticated thermal-stress models to calculate temperatures, stresses, and shrinkage, including the formation of an air gap near the corners, and its effect on heat flow across the mold / shell interface.

Discussion

This spreadsheet finite difference model was very easy to create and equally easy to modify. This is attributed mainly to the strong correspondence between the program (finite difference

equations), input data, and results all being stored in the same place (the spreadsheet cells) in an intuitive manner. This was achieved by ensuring that each nodal equation occupies a single cell in the spread sheet, which has the added advantage of better computational efficiency. This benefit should apply to any two-variable problem, including both 2-D steady state and 1-D transient problems, as in the present example.

The simplicity of this model is important because most of the uses of the model required modifications that were not originally anticipated. The spreadsheet model was easier to work with than FORTRAN programs in this regard.

Conclusions

A commercial spreadsheet program, such as Excel or WINGZ on a personal computer is a powerful tool that can be used to develop surprisingly sophisticated mathematical models. It offers the advantage over traditional compiled language programs of simplicity in all phases of model development, program modification, running the model and examining the results. This is especially evident in heat flow calculations where each cell can represent a single node in the simulation.

Cell equations are presented in the present paper which incorporate simple, robust numerical methods to calculate 2-D steady state heat conduction and 1-D transient solidification. They are used to construct a coupled thermal model of the continuous casting of steel slabs, including the water-cooled copper mold, the solidifying steel shell, and the interface between them. Versions of this model are being applied to aid in the understanding of various aspects of this process.

Acknowledgments

The authors wish to thank Inland Steel, Armco Inc., LTV Steel, BHP Steel, and the National Science Foundation (Grant # MSS-89567195-PYI) for funding which made this work possible, and Vaughn Voller for valuable discussions.

References

Burmeister, L. C., 1983, *Convective Heat Transfer*, John Wiley & Sons, New York, pp. 484-486.

Carslaw, H. S., and J. C. Jaeger, 1959, *Conduction of Heat in Solids*, Oxford University Press, 2nd ed., pp. 285-291.

Hills, A. W. D., 1969, "The Generalized Integral Profile Method for the Analysis of Unidirectional Heat Flow during Solidification", *Trans. TMS-AIME*, Vol 245, p. 1471.

Ho, B., 1992, "Characterization of Interfacial Heat Transfer in the Continuous Slab Casting Process", Masters Thesis, University of Illinois, Urbana, IL.

Jenkins, M.S., Thomas, B.G., Chen, W.C., and Mahapatra, R.B., 1994, "Investigation of Strand Surface Defects Using Mold Instrumentation and Modeling", *Steelmaking Conference Proceedings,* Vol. 77, Iron and Steel Society, Warrendale, PA.

Lait, J.E., J.K. Brimacombe, and F. Weinberg, 1974, "Mathematical modeling of heat flow in the continuous casting of steel", *Ironmaking and Steelmaking*, No. 2, pp. 90-97.

Mahapatra, R.B., J.K. Brimacombe and I.V. Samarasekera, "Mold Behavior and its Influence on Quality in the Continuous Casting of Slabs: Part I. Industiral Trials, Mold Temperature Measurements, and Mathematical Modelling," *Metallurgical Transactions B*, Vol. 22B (6), 1991, 861-874.

Minkowycz, W. J., E. M. Sparrow, G. E. Schneider, and R. H. Pletcher, 1988, *Handbook of Numerical Heat Transfer*, John Wiley & Sons, Inc., New York, pp. 69-71.

Szekely, J., Evans, J., and Brimacombe, J.K., 1988, *The Mathematical and Physical Modeling of Primary Metals Processing Operations,* John Wiley and Sons, New York, pp. 203-216.

Thomas, B.G., 1989, "Application of Mathematical Models to the Continuous Slab Casting Mold", *Iron and Steel Society Transactions*, Vol. 16, No. 12, pp. 53-66.

Table I Stainless steel slab solidification test problem

Input data	Lait et al. 1974	Spreadsheet Model
Slab size	127 x 1090 mm	N/A
Mold length, L	510 mm (effective)	510 mm
Thermal conductivity, k	15.9 + 0.0115 T(˚C)	34 W/m K
Specific heat, Cp	682 J/kgK	682 J/kgK
Latent heat, L_f	272 J/g	272 J/g
Density, ρ	7400 kg/m^3	7400 kg / m^3
Solidus temp, T_{sol}	1399 ˚C	1399 ˚C
Liquidus temp, T_{liq}	1460 ˚C	1399 ˚C
Pour temp, T_{pour}	1480 ˚C	1419 ˚C
Superheat	20 ˚C	20 ˚C
Casting speed, v	165 mm/s	165 mm/s
Time data	N / A	0,6,10,25,40 s
Heat flux data, q", MW/m^2	q (W/m^2) = 2.68 - .335 $\sqrt{t\,(s)}$	2.68, 1.86, 1.62, 1.00, 0.56
Time step size, Δt		0.2 s
Mesh size, Δx		2 mm

Appendix I Cell Equations

Mold Temperatures

1. Interior Node (2-D) $$T_{cell} = \frac{T_W\,\Delta y^2 + T_E\,\Delta y^2 + T_S\,\Delta x^2 + T_N\,\Delta x^2}{2(\Delta y^2 + \Delta x^2)}$$

2. (1-D) $$T_{cell} = \frac{1}{2}(T_W + T_E)$$

Cold Face with Convection Boundary Conditions

3. (2-D) $$T_{cell} = \frac{T_S\,\Delta x^2 + T_N\,\Delta x^2 + 2T_E\,\Delta y^2 + \frac{2h_{water}\,\Delta x \Delta y^2}{k}\,T_{water}}{2\Delta y^2 + 2\Delta x^2 + \frac{2h_{water}\,\Delta x\,\Delta y^2}{k}}$$

4. (1-D) $$T_{cell} = \frac{T_E + \frac{h_{water}\,\Delta x}{k}\,T_{water}}{1 + \frac{h_{water}\,\Delta x}{k}}$$

Hot Face with Heat Flux Boundary Conditions

5. (2-D) $$T_{cell} = \frac{T_N\,\Delta x^2 + T_S\,\Delta x^2 + 2T_W\,\Delta y^2 + \frac{2q''\,\Delta x \Delta y^2}{k}}{2\Delta x^2 + 2\Delta y^2}$$

6. (1-D) $$T_{cell} = T_W + \frac{q''\,\Delta x}{k}$$

7. Top Row of Mold with Convection Boundary Conditions

(2-D) $$T_{cell} = \frac{T_W\,\Delta y^2 + T_E\,\Delta y^2 + 2T_S\,\Delta x^2 + \frac{2h_\infty\,\Delta x^2 \Delta y}{k}\,T_\infty}{2\Delta y^2 + 2\Delta x^2 + \frac{2h_\infty\,\Delta x^2 \Delta y}{k}}$$

8. Corner Cold Face Node with Convection to Ambient, h_∞, and Water, h_{water}

$$T_{cell} = \frac{\frac{h_\infty\,\Delta x^2 \Delta y}{k}\,T_\infty + \frac{h_{water}\,\Delta y^2 \Delta x}{k}\,T_{water} + T_E \Delta y^2 + T_S \Delta x^2}{\frac{h_\infty\,\Delta x^2 \Delta y}{k} + \frac{h_{water}\,\Delta y^2 \Delta x}{k} + \Delta y^2 + \Delta x^2}$$

9. Corner Hot Face Node with Convection to Ambient and Flux Boundary Conditions

$$T_{cell} = \frac{\frac{h_\infty\,\Delta x^2 \Delta y}{k}\,T_\infty + \frac{q''\Delta x \Delta y^2}{k} + T_W \Delta y^2 + T_S \Delta x^2}{\frac{h_\infty\,\Delta x^2 \Delta y}{k} + \Delta y^2 + \Delta x^2}$$

Solidifying Steel Enthalpies

10. Meniscus nodes (Top row) $$H_{cell} = C_p * T_{pour} + L_f * \mathrm{int}\left(\frac{T_{pour}}{T_{sol}}\right)$$

11. Surface Node $$H_{cell} = H_N + \frac{2k\Delta t}{\rho \Delta x^2}\left(\min\left[\frac{H_{NE}}{C_p}, \max\left\{\frac{H_{NE}-L_f}{C_p}, T_{sol}\right\}\right] - \min\left[\frac{H_N}{C_p}, \max\left\{\frac{H_N - L_f}{C_p}, T_{sol}\right\}\right]\right) - \frac{2q''\Delta t}{\rho \Delta x}$$

12. All other nodes $$H_{cell} = H_N + \frac{k\Delta t}{\rho \Delta x^2}\left(\min\left[\frac{H_{NE}}{C_p}, \max\left\{\frac{H_{NE} - L_f}{C_p}, T_{sol}\right\}\right] - 2\min\left[\frac{H_N}{C_p}, \max\left\{\frac{H_N - L_f}{C_p}, T_{sol}\right\}\right] + \min\left[\frac{H_{NW}}{C_p}, \max\left\{\frac{H_{NW} - L_f}{C_p}, T_{sol}\right\}\right]\right)$$

Centerline nodes are the same as interior nodes except that $H_{NE} = H_{NW}$.

Solidifying Steel Temperatures

13. Meniscus nodes (Top row) $T_{cell} = T_{pour}$

14. All other nodes: $$T_{cell} = \frac{H_{cell} - \max\left(0, \min\left[L_f, H_{cell} - T_{sol}*C_p\right]\right)}{C_p}$$

Figures

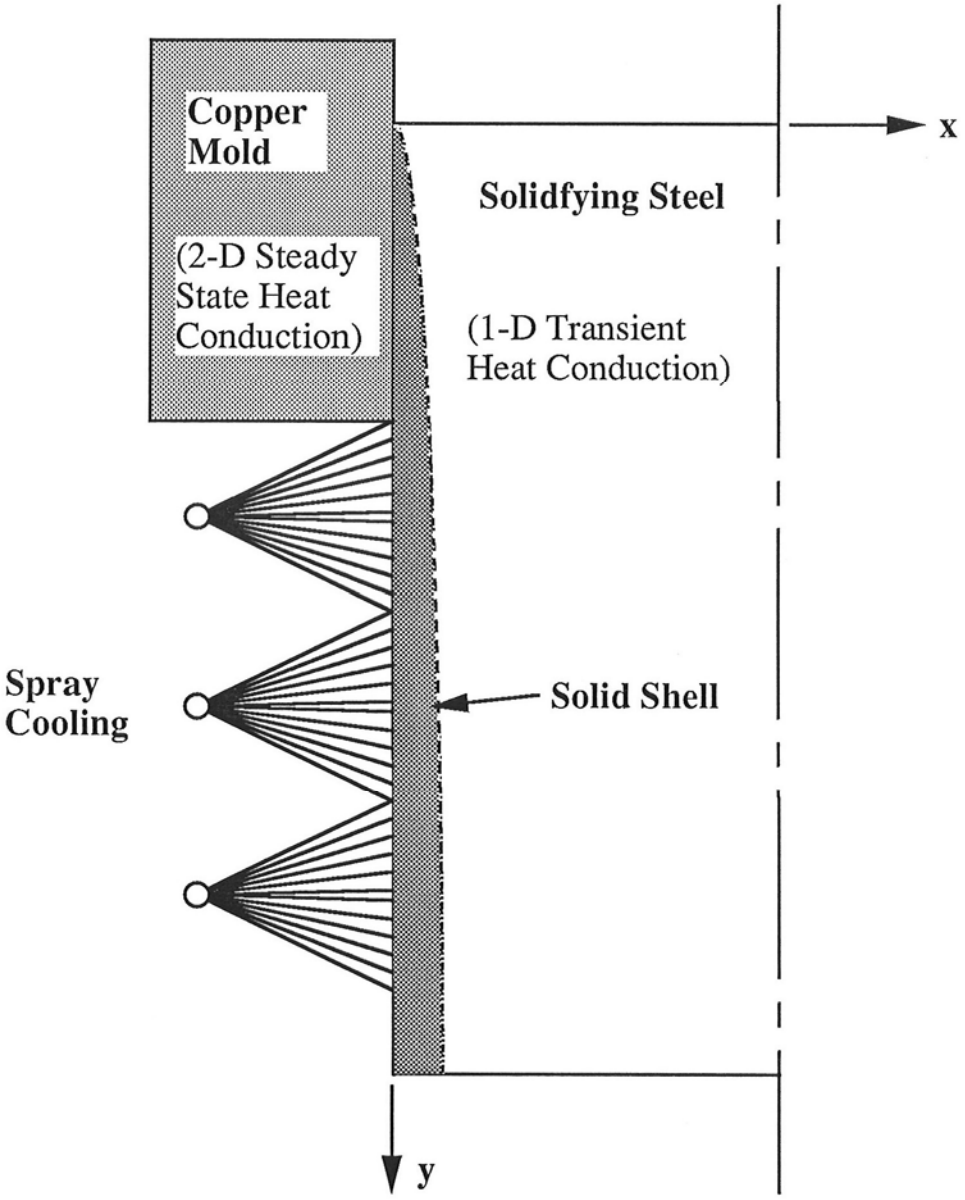

Figure 1 Schematic of model domain

Figure 2 Spreadsheet model of continuous casting

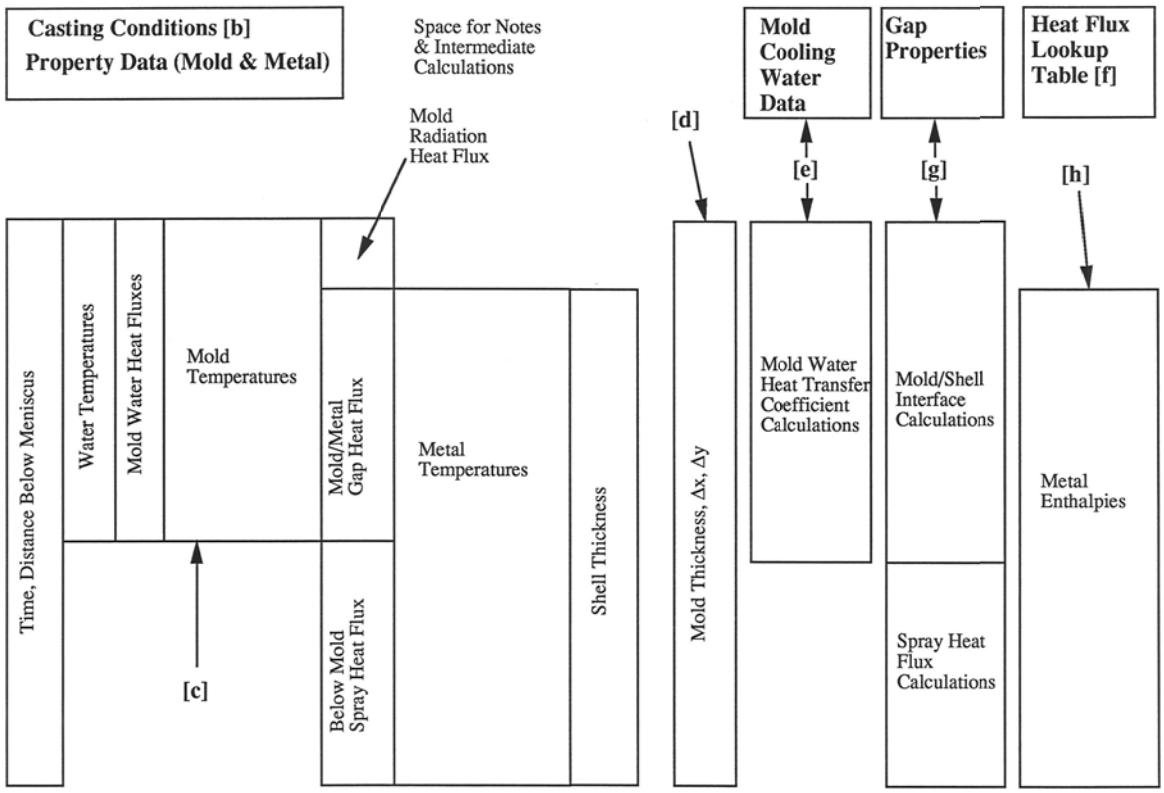

Figure 2 a) Overall structure

Casting Conditions		
Casting Speed (m/min.)	**1.0**	
Meniscus Depth from Top (mm)	**100**	
Pouring Temperature (°C)	**1519**	
Initial Cooling Water Temperature (°C)	**20**	
Ambient Temperature (°C)	**25**	
Mold Length (mm)	**700**	
Mold Thickness (at top) (mm)	**35**	
Machine Radius (m)	**10.5**	
Property Data	**Mold**	**Metal**
Thermal Conductivity (W/mK)	**335**	**29.7**
Density (kg/m^3)	**8700**	**7200**
Specific Heat (kJ/kgK)	**0.8368**	**0.6820**
Latent Heat of Fusion (KJ/kg)		**272.0**
Solidification Temperature (°C)		**1503**
Convection Coefficient (Top of mold) (m^2K/W)	**0.001**	
Thermal Diffusivity (m^2/s)	4.60E+07	6.05E+06
Δt (s)		**0.2**
Δx (mm)	7	**2**
Δy (mm)	5	
Δt/Δx^2 (s/mm^2)	4.082E-03	0.05
aΔt/Δx^2 (s/mm^2)	0.19	0.30

Bold = Data input by user

Figure 2 b) Input data section

Time (s)	Dist Below Men. (mm)	Water T (°C)	Heat Flux (MW/m^2)	Cold face 35.0	Mold 2 28.0	Mold 3 21.0	Mold 4 14.0	Mold 5 7.0	Hot Face 0.0	Heat Flux (MW/m^2)	Metal Surf. 0.0	Metal 2 2.0	Metal 3 4.0	....	Shell (mm)	Integral Profile
-6.0	-100	33.5	0.075	35.6	37.3	38.8	39.9	40.7	40.9	0.00008						
-4.8	-80	33.5	0.107	36.4	38.8	40.8	42.3	43.3	43.7	0.00010						
-3.6	-60	33.4	0.186	38.6	42.6	46.1	48.8	50.6	51.3	0.00014						
-2.4	-40	33.4	0.350	42.9	50.3	57.0	62.5	66.3	67.9	0.00025						
-1.2	-20	33.3	0.639	50.2	63.8	76.9	89.2	99.4	105.1	0.00057						
0.0	0	33.2	1.003	58.9	80.5	104.4	132.5	168.2	217.8	2.417	1519.0	1519.0	1519.0	....	0.00	0.00
0.3	5	33.1	1.216	63.8	89.8	118.5	151.8	192.7	246.0	2.334	1503.0	1519.0	1519.0	....	0.41	0.45
0.6	10	33.0	1.404	67.9	97.7	130.2	167.2	211.0	264.0	2.306	1503.0	1514.2	1519.0	....	0.68	0.76
0.9	15	33.0	1.563	71.4	104.3	139.7	179.2	224.5	277.2	2.286	1503.0	1512.2	1517.5	....	0.92	1.03
1.2	20	32.9	1.695	74.2	109.6	147.2	188.3	234.3	286.6	2.272	1503.0	1511.1	1516.4	....	1.15	1.28
1.5	25	32.8	1.801	76.4	113.7	152.9	194.9	240.8	291.6	2.207	1480.2	1510.2	1515.4	....	1.36	1.52
1.8	30	32.7	1.886	78.1	116.9	157.2	199.7	244.7	292.2	2.048	1414.9	1503.0	1514.6	....	1.55	1.74
2.1	35	32.6	1.952	79.5	119.3	160.4	203.1	247.6	293.5	1.981	1387.5	1503.0	1512.0	....	1.74	1.95
2.4	40	32.5	2.005	80.5	121.1	162.8	205.6	249.8	295.2	1.956	1377.7	1503.0	1510.8	....	1.93	2.16
2.7	45	32.4	2.046	81.3	122.5	164.6	207.6	251.7	296.7	1.946	1374.3	1503.0	1510.0	....	2.11	2.36
3.0	50	32.3	2.079	81.9	123.6	165.9	209.1	253.1	298.1	1.941	1373.1	1503.0	1509.4	....	2.28	2.55
~	~	~	~	~	~	~	~	~	~	~	~	~	~	~	~	~
39.0	650	20.8	1.505	61.6	91.7	122.0	152.6	183.5	214.8	1.351	1029.8	1118.3	1201.3	....	15.61	17.48
39.3	655	20.7	1.490	61.2	91.1	121.3	151.8	182.6	213.9	1.349	1028.4	1116.7	1199.4	....	15.70	17.58
39.6	660	20.6	1.473	60.7	90.5	120.5	150.8	181.6	212.8	1.348	1026.9	1115.0	1197.4	....	15.79	17.68
39.9	665	20.5	1.455	60.2	89.8	119.6	149.8	180.4	211.6	1.347	1025.3	1113.3	1195.4	....	15.88	17.78
40.2	670	20.5	1.434	59.7	88.9	118.5	148.5	179.1	210.3	1.346	1023.7	1111.5	1193.4	....	15.97	17.88
40.5	675	20.4	1.410	59.1	88.0	117.3	147.1	177.6	208.7	1.345	1022.0	1109.7	1191.4	....	16.05	17.98
40.8	680	20.3	1.383	58.4	86.9	115.8	145.4	175.7	206.9	1.345	1020.3	1107.9	1189.4	....	16.14	18.08
41.1	685	20.3	1.350	57.5	85.5	114.1	143.4	173.6	204.7	1.345	1018.5	1106.1	1187.4	....	16.23	18.18
41.4	690	20.2	1.309	56.5	84.0	112.1	141.1	171.0	202.1	1.345	1016.7	1104.2	1185.4	....	16.32	18.28
41.7	695	20.1	1.255	55.1	82.1	109.8	138.3	167.9	198.9	1.346	1014.8	1102.3	1183.5	....	16.41	18.38
42.0	700	20.1	1.166	52.9	79.8	107.1	135.0	164.1	194.5	1.349	1012.8	1100.4	1181.5	....	16.50	18.48

Figure 2 c) Main section of mold and shell models

Mold Thickness (mm)	Δx (mm)	Δy (mm)
38.812	7.7625	20.00
37.974	7.5947	20.00
37.173	7.4346	20.00
36.410	7.2821	20.00
35.686	7.1372	20.00
35.000	7.0000	12.50
34.834	6.9669	5.00
34.671	6.9343	5.00
34.510	6.9021	5.00
34.352	6.8704	5.00
34.196	6.8392	5.00
34.042	6.8085	5.00
33.891	6.7782	5.00
33.742	6.7484	5.00
33.596	6.7191	5.00
33.452	6.6903	5.00
~	~	~
33.452	6.6903	5.00
33.596	6.7191	5.00
33.742	6.7484	5.00
33.891	6.7782	5.00
34.042	6.8085	5.00
34.196	6.8392	5.00
34.352	6.8704	5.00
34.510	6.9021	5.00
34.671	6.9343	5.00
34.834	6.9669	5.00
35.000	7.0000	5.00

Figure 2 d) Mesh size definition section

Convective Heat Transfer Coefficients (Sleicher & Rouse)	
No boiling 10e3<Re<120e3 l/D>60 (fully developed) .7<Pr<120	Channel geometry Depth (mm) 25 Width (mm) 6
Hydraulic diameter (mm) 9.68 Water flow rate (m^3/s) 5.88E-04 Water flow rate (l/min.) 35.31 Water velocity (m/s) 9.00 Mass flow rate (m^3/s) 1.35	

Film Temp. (°C)	Density (kg/m^3)	k,water (W/mK)	Cp,water (J/kgK)	Viscosity (Pa-s)	Pr,water	Re,water	h (W/m^2K)
34.50	994.2	0.623	4179.33	0.00077	5.18	1.12E+05	3.58E+04
34.93	994.0	0.623	4179.12	0.00077	5.13	1.13E+05	3.59E+04
35.99	993.7	0.623	4178.61	0.00075	5.02	1.15E+05	3.62E+04
38.14	993.0	0.623	4177.68	0.00072	4.80	1.20E+05	3.68E+04
41.77	991.7	0.623	4176.44	0.00067	4.45	1.28E+05	3.78E+04
46.05	990.0	0.623	4175.50	0.00062	4.08	1.39E+05	3.90E+04
48.41	989.0	0.623	4175.21	0.00060	3.89	1.45E+05	3.96E+04
50.46	988.1	0.623	4175.10	0.00057	3.74	1.50E+05	4.02E+04
52.16	987.4	0.623	4175.11	0.00056	3.62	1.54E+05	4.06E+04
53.52	986.8	0.623	4175.18	0.00054	3.53	1.58E+05	4.10E+04
54.58	986.3	0.623	4175.27	0.00053	3.46	1.61E+05	4.13E+04
55.40	985.9	0.623	4175.36	0.00053	3.40	1.63E+05	4.15E+04
56.01	985.6	0.623	4175.45	0.00052	3.36	1.65E+05	4.17E+04
56.48	985.3	0.623	4175.52	0.00052	3.33	1.66E+05	4.18E+04
56.82	985.2	0.622	4175.58	0.00051	3.31	1.67E+05	4.19E+04
57.08	985.0	0.622	4175.62	0.00051	3.30	1.68E+05	4.19E+04
~	~	~	~	~	~	~	~
41.15	991.9	0.611	4176.63	0.00068	4.51	1.27E+05	3.69E+04
40.91	992.0	0.611	4176.70	0.00068	4.53	1.26E+05	3.68E+04
40.65	992.1	0.611	4176.78	0.00069	4.55	1.26E+05	3.67E+04
40.37	992.2	0.611	4176.87	0.00069	4.58	1.25E+05	3.66E+04
40.06	992.3	0.610	4176.98	0.00070	4.61	1.24E+05	3.66E+04
39.72	992.4	0.610	4177.10	0.00070	4.64	1.24E+05	3.65E+04
39.33	992.6	0.610	4177.23	0.00070	4.68	1.23E+05	3.64E+04
38.87	992.7	0.610	4177.40	0.00071	4.72	1.22E+05	3.62E+04
38.33	992.9	0.610	4177.61	0.00072	4.78	1.20E+05	3.61E+04
37.61	993.2	0.610	4177.90	0.00073	4.85	1.19E+05	3.59E+04
36.45	993.5	0.610	4178.40	0.00074	4.97	1.16E+05	3.56E+04

Figure 2 e) Cooling water convection section

Look-up table	
Distance Below Meniscus(mm)	q (MW/m^2)
-100	0.000
-20	1.000
0	2.680
75	2.209
100	2.136
175	1.961
250	1.820
325	1.700
450	1.526
600	1.348
700	1.231

Figure 2 f) Interfacial heat flux look - up table

Gap Properties	
h,contact (mold/flux)(W/m^2K)	1.00E+09
h,contact (flux/shell)(W/m^2K)	1.00E+09
Contact Resistance (m^2K/W) (mold/flux)	1.00E-09
Contact Resistance (m^2K/W) (flux/shell)	1.00E-09
Emissivity (-)	0.80
Kpowder,s (W/mK)	0.60
Kpowder,l (W/mK)	0.50
K,air (W/mK)	0.06
Tcrystallization (°C)	1020

d,solid flux (mm)	d,molten flux (mm)	d,air (mm)	Conduction (m^2K/W)	Radiation (m^2K/W)	Gap Resistance (m^2K/W)	Gap h (W/m^2K)
				1.9230E-01		
				1.8971E-01		
				1.8267E-01		
				1.6838E-01		
				1.4073E-01		
0.4000	0.0000	0.0000	6.6667E-04	2.7976E-03	5.3837E-04	1857.45
0.4000	0.0000	0.0000	6.6667E-04	2.8059E-03	5.3868E-04	1856.38
0.4000	0.0000	0.0000	6.6667E-04	2.7687E-03	5.3729E-04	1861.18
0.4000	0.0000	0.0000	6.6667E-04	2.7417E-03	5.3627E-04	1864.74
0.4000	0.0000	0.0000	6.6667E-04	2.7225E-03	5.3553E-04	1867.30
0.4000	0.0000	0.0000	6.6667E-04	2.8041E-03	5.3861E-04	1856.62
0.4000	0.0000	0.0000	6.6667E-04	3.0881E-03	5.4830E-04	1823.82
0.4000	0.0000	0.0000	6.6667E-04	3.2161E-03	5.5220E-04	1810.94
0.4000	0.0000	0.0000	6.6667E-04	3.2604E-03	5.5349E-04	1806.71
0.4000	0.0000	0.0000	6.6667E-04	3.2734E-03	5.5387E-04	1805.49
0.4000	0.0000	0.0000	6.6667E-04	3.2757E-03	5.5393E-04	1805.28
~	~	~	~	~	~	~
0.4000	0.0000	0.0000	6.6667E-04	6.3620E-03	6.0343E-04	1657.18
0.4000	0.0000	0.0000	6.6667E-04	6.3861E-03	6.0365E-04	1656.59
0.4000	0.0000	0.0000	6.6667E-04	6.4116E-03	6.0388E-04	1655.96
0.4000	0.0000	0.0000	6.6667E-04	6.4388E-03	6.0412E-04	1655.31
0.4000	0.0000	0.0000	6.6667E-04	6.4681E-03	6.0437E-04	1654.60
0.4000	0.0000	0.0000	6.6667E-04	6.4996E-03	6.0465E-04	1653.85
0.4000	0.0000	0.0000	6.6667E-04	6.5340E-03	6.0494E-04	1653.04
0.4000	0.0000	0.0000	6.6667E-04	6.5716E-03	6.0527E-04	1652.17
0.4000	0.0000	0.0000	6.6667E-04	6.6132E-03	6.0562E-04	1651.21
0.4000	0.0000	0.0000	6.6667E-04	6.6604E-03	6.0601E-04	1650.14
0.4000	0.0000	0.0000	6.6667E-04	6.7182E-03	6.0648E-04	1648.85

Figure 2 g) Interfacial heat transfer section

Metal Surface 0.0	Metal 2 2.0	Metal 3 4.0	Metal 4 6.0	Metal 5 8.0	Metal 6 10.0	Metal 7 12.0	Metal 8 14.0	Metal 9 16.0	Metal 10 18.0	Metal 11 20.0
1.30791	1.30791	1.30791	1.30791	1.30791	1.30791	1.30791	1.30791	1.30791	1.30791	1.30791
1.24308	1.30791	1.30791	1.30791	1.30791	1.30791	1.30791	1.30791	1.30791	1.30791	1.30791
1.18563	1.30461	1.30791	1.30791	1.30791	1.30791	1.30791	1.30791	1.30791	1.30791	1.30791
1.12673	1.30330	1.30691	1.30791	1.30791	1.30791	1.30791	1.30791	1.30791	1.30791	1.30791
1.06744	1.30248	1.30612	1.30760	1.30791	1.30791	1.30791	1.30791	1.30791	1.30791	1.30791
1.00946	1.30192	1.30547	1.30725	1.30781	1.30791	1.30791	1.30791	1.30791	1.30791	1.30791
0.96498	1.29679	1.30493	1.30688	1.30767	1.30788	1.30791	1.30791	1.30791	1.30791	1.30791
0.94627	1.28103	1.30312	1.30653	1.30749	1.30782	1.30790	1.30791	1.30791	1.30791	1.30791
0.93958	1.25906	1.30230	1.30579	1.30730	1.30775	1.30788	1.30790	1.30791	1.30791	1.30791
0.93723	1.23481	1.30175	1.30519	1.30698	1.30765	1.30785	1.30790	1.30791	1.30791	1.30791
0.93643	1.20969	1.30135	1.30469	1.30664	1.30751	1.30780	1.30788	1.30790	1.30791	1.30791
~	~	~	~	~	~	~	~	~	~	~
0.70235	0.76266	0.81931	0.87159	0.91849	0.95916	0.99394	1.25381	1.29732	1.29756	1.29765
0.70135	0.76155	0.81799	0.86996	0.91661	0.95738	0.99283	1.24451	1.29730	1.29752	1.29760
0.70032	0.76041	0.81664	0.86835	0.91483	0.95577	0.99185	1.23486	1.29727	1.29747	1.29755
0.69926	0.75924	0.81527	0.86677	0.91315	0.95430	0.99097	1.22490	1.29725	1.29744	1.29750
0.69816	0.75805	0.81390	0.86522	0.91157	0.95295	0.99018	1.21468	1.29723	1.29740	1.29746
0.69702	0.75683	0.81253	0.86372	0.91007	0.95169	0.98946	1.20420	1.29721	1.29737	1.29742
0.69585	0.75558	0.81116	0.86225	0.90864	0.95053	0.98880	1.19351	1.29719	1.29734	1.29739
0.69463	0.75433	0.80981	0.86083	0.90728	0.94943	0.98818	1.18261	1.29718	1.29731	1.29736
0.69338	0.75305	0.80846	0.85945	0.90598	0.94840	0.98761	1.17151	1.29716	1.29728	1.29733
0.69208	0.75176	0.80712	0.85810	0.90474	0.94743	0.98707	1.16024	1.29715	1.29726	1.29730
0.69071	0.75046	0.80580	0.85679	0.90354	0.94651	0.98656	1.14881	1.29714	1.29724	1.29728

Figure 2 h) Shell enthalpy section

NW	N	NE
W	cell	E
	S	

Figure 3 Subscript nomenclature used in equations to define relative position of cells

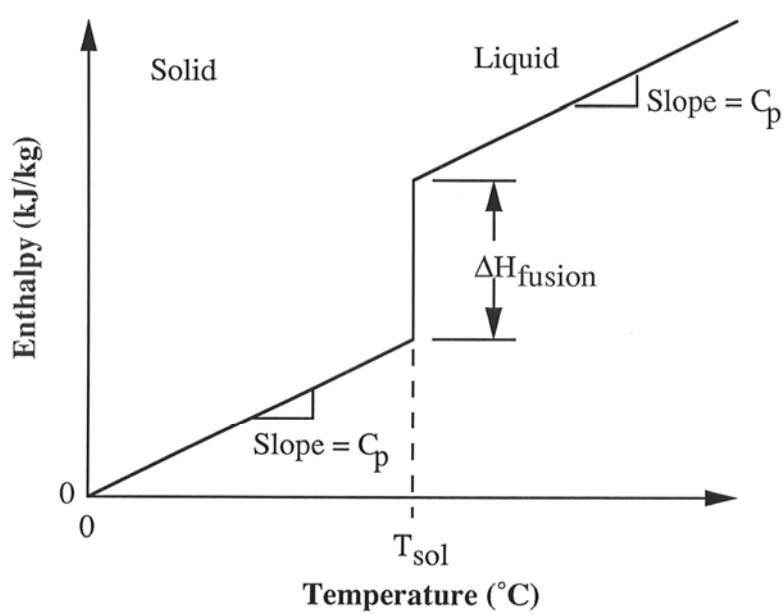

Figure 4 Temperature - enthalpy relationship assumed in the solidification model

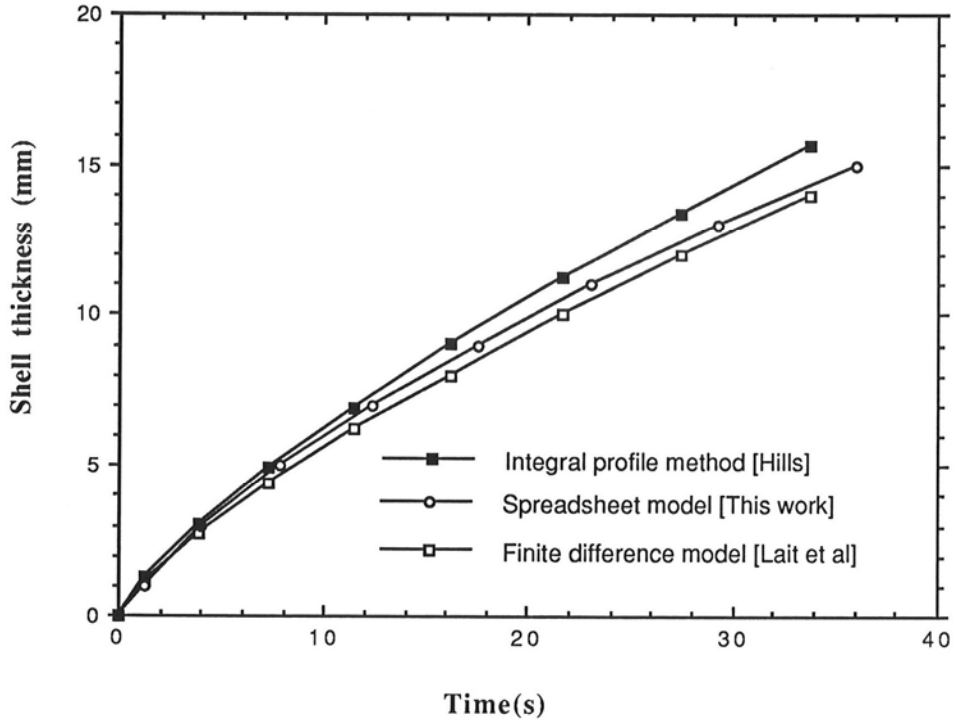

Figure 5 Comparison of spreadsheet model predictions with previous models.

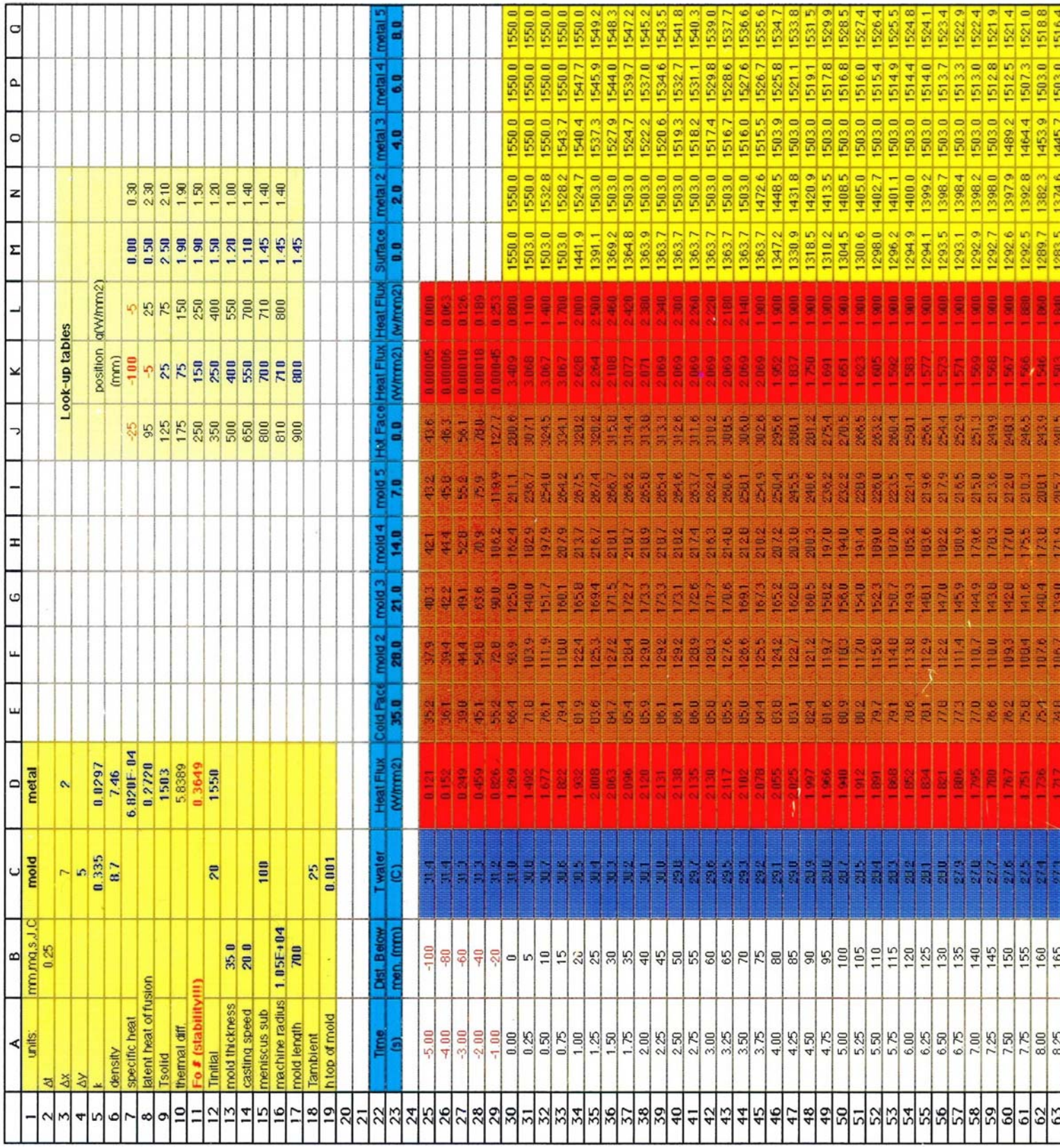

	A	B	C	D	E	F	G	H	I	J	K	L	M	N	O	P	Q
1	units:	mm,mg,s,J,C	mold	metal													
2	Δt	0.25															
3	Δx		7	2													
4	Δy		5														
5	k		0.335	0.0297													
6	density		8.7	7.46													
7	specific heat			6.820E-04													
8	latent heat of fusion			0.2720													
9	Tsolid			1503													
10	thermal diff.			5.8389													
11	Fo # (stability!!!)			0.3649													
12	Tinitial		20	1550													
13	mold thickness	35.0															
14	casting speed	20.0															
15	meniscus sub		100														
16	machine radius	1.05E+04															
17	mold length	700															
18	Tambient		25														
19	h top of mold		0.001														
20											Look-up tables						
21											position (mm)	q(W/mm2)					
22	Time (s)	Dist. Below men. (mm)	T water (C)	Heat Flux (W/mm2)	Cold Face	mold 2	mold 3	mold 4	mold 5	Hot Face	Heat Flux (W/mm2)	Heat Flux (W/mm2)	Surface	metal 2	metal 3	metal 4	metal 5
23					35.0	28.0	21.0	14.0	7.0	0.0	-25	-0.00	0.0	2.0	4.0	6.0	8.0
24											-100	-0.30					
25	-5.00	-100	30.4	0.121	35.2	37.9	40.3	42.1	43.2	43.6	-5	-0.50					
26	-4.00	-80	30.4	0.152	36.1	39.4	42.2	44.4	45.8	46.3	25	-2.30					
27	-3.00	-60	30.3	0.249	39.0	44.4	49.1	52.8	55.2	56.1	75	-2.10					
28	-2.00	-40	30.3	0.459	45.1	54.0	63.6	70.9	75.9	78.0	150	-1.90					
29	-1.00	-20	30.2	0.826	55.2	72.8	90.0	106.2	119.9	127.7	250	-1.50					
30	0.00	0	30.0	1.269	66.4	93.9	125.0	162.4	211.1	280.6	400	-1.20	1550.0	1550.0	1550.0	1550.0	1550.0
31	0.25	5	30.0	1.492	71.0	103.9	140.0	182.9	236.7	307.1	550	-1.00	1503.0	1550.0	1550.0	1550.0	1550.0
32	0.50	10	30.0	1.677	76.1	111.9	151.7	197.9	254.0	324.5	700	-1.10	1503.0	1532.8	1550.0	1550.0	1550.0
33	0.75	15	30.0	1.822	79.4	118.0	160.1	207.9	264.2	334.1	710	-1.45	1503.0	1528.2	1543.7	1550.0	1550.0
34	1.00	20	30.0	1.932	81.9	122.4	165.8	213.7	267.5	328.2	800	-1.40	1441.9	1524.7	1540.4	1547.7	1550.0
35	1.25	25	30.0	2.008	83.6	125.3	169.4	216.7	267.4	320.2	810	-1.45	1391.1	1503.0	1537.3	1545.9	1549.2
36	1.50	30	30.0	2.063	84.7	127.2	171.5	218.1	266.7	315.0	900	-1.45	1369.2	1503.0	1527.9	1544.0	1548.3
37	1.75	35	30.0	2.096	85.4	128.4	172.7	218.7	266.2	314.4			1364.8	1503.0	1524.7	1539.7	1547.2
38	2.00	40	30.0	2.120	85.9	129.0	173.3	218.9	265.8	313.0			1363.9	1503.0	1522.2	1537.0	1545.2
39	2.25	45	30.0	2.131	86.1	129.2	173.3	218.7	265.4	313.3			1363.7	1503.0	1520.6	1534.6	1543.5
40	2.50	50	29.9	2.138	86.1	129.2	173.1	218.2	264.6	312.6			1363.7	1503.0	1519.3	1532.7	1541.8
41	2.75	55	29.7	2.135	86.0	128.9	172.6	217.4	263.7	311.6			1363.7	1503.0	1518.2	1531.1	1540.3
42	3.00	60	29.6	2.130	85.8	128.3	171.7	216.3	262.4	310.2			1363.7	1503.0	1517.4	1529.8	1539.0
43	3.25	65	29.5	2.117	85.5	127.6	170.6	214.8	260.6	308.5			1363.7	1503.0	1516.7	1528.6	1537.7
44	3.50	70	29.3	2.102	85.0	126.6	169.1	212.8	258.1	306.0			1363.7	1503.0	1516.0	1527.6	1536.6
45	3.75	75	29.2	2.078	84.4	125.5	167.3	210.2	254.9	302.6			1363.7	1472.6	1515.5	1526.7	1535.6
46	4.00	80	29.1	2.055	83.8	124.2	165.2	207.2	250.4	299.6			1347.2	1448.5	1503.9	1525.8	1534.7
47	4.25	85	29.0	2.025	83.1	122.7	162.8	203.8	245.5	296.1			1330.9	1431.8	1503.0	1521.1	1533.8
48	4.50	90	29.0	1.997	82.4	121.2	160.5	200.3	240.6	291.2			1318.5	1420.9	1503.0	1519.1	1531.5
49	4.75	95	29.0	1.966	81.6	119.7	158.2	197.0	236.2	275.4			1310.2	1413.5	1503.0	1517.8	1529.9
50	5.00	100	29.0	1.940	80.9	118.0	156.0	194.0	232.2	270.5			1304.5	1408.5	1503.0	1516.8	1528.5
51	5.25	105	29.5	1.912	80.2	117.0	154.0	191.4	228.9	266.5			1300.6	1405.0	1503.0	1516.0	1527.4
52	5.50	110	29.4	1.891	79.7	115.8	152.3	189.0	226.0	263.2			1298.0	1402.7	1503.0	1515.4	1526.4
53	5.75	115	29.3	1.868	79.1	114.8	150.7	187.0	223.5	260.4			1296.2	1401.1	1503.0	1514.9	1525.5
54	6.00	120	29.2	1.852	78.6	113.8	149.3	185.2	221.4	258.1			1294.9	1400.0	1503.0	1514.4	1524.8
55	6.25	125	29.1	1.834	78.1	112.9	148.1	183.6	219.6	256.1			1294.1	1399.2	1503.0	1514.0	1524.1
56	6.50	130	29.0	1.821	77.8	112.2	147.0	182.2	217.9	254.4			1293.5	1398.7	1503.0	1513.7	1523.4
57	6.75	135	27.9	1.806	77.3	111.4	145.9	180.9	216.5	252.9			1293.1	1398.4	1503.0	1513.3	1522.9
58	7.00	140	27.8	1.795	77.0	110.7	144.9	179.6	215.0	251.5			1292.9	1398.2	1503.0	1513.0	1522.4
59	7.25	145	27.7	1.780	76.6	110.0	143.8	178.3	213.6	249.9			1292.7	1398.0	1503.0	1512.8	1521.9
60	7.50	150	27.6	1.767	76.2	109.3	142.8	177.0	212.0	248.3			1292.6	1397.9	1489.2	1512.5	1521.4
61	7.75	155	27.5	1.751	75.8	108.4	141.6	175.5	210.3	246.5			1292.5	1392.8	1464.4	1507.3	1521.0
62	8.00	160	27.4	1.736	75.4	107.6	140.4	173.8	208.1	243.9			1289.7	1382.3	1453.9	1503.0	1518.8
63	8.25	165	[illegible]	[illegible]	[illegible]	[illegible]	[illegible]	[illegible]	[illegible]	[illegible]			[illegible]	[illegible]	[illegible]	[illegible]	[illegible]

Scan of actual spread-sheet page, with sections colored according to function (blue=water, read=h, brown=copper, yellow=solidifying steel.